

SUPPORTING INFORMATION

TITLE. Altered protein dynamics and increased aggregation in human γ S-crystallin due to cataract-associated deamidations

AUTHORS. Heather M. Forsythe¹, Calvin J. Vetter², Kayla Ann Jara¹, Patrick N. Reardon³, Larry L. David⁴, Elisar J. Barbar^{1*} and Kirsten J. Lampi^{2*}

PAGES- 10

SUPPORTING FIGURES and TABLE

Figure S1. Chromatograms of doubly charged γ S peptide 7-18 (ITFYEDKNFQGR).

Figure S2. Light scattering of γ S crystallins.

Figure S3. Summary of NMR methods.

Figure S4. TROSY overlay of WT (black) with N14D (cyan) on the left, and N76D (red) on the right.

Figure S5. CLEANEX (top) and day 6 core residue (bottom) intensities of WT (black), N14D (cyan), and N76D (red).

Figure S6. NOE values for WT (grey), N14D (cyan), and N76D (red).

Table S1. Measured H/D exchange rates for WT (grey), N14D (cyan), and N76D (red).

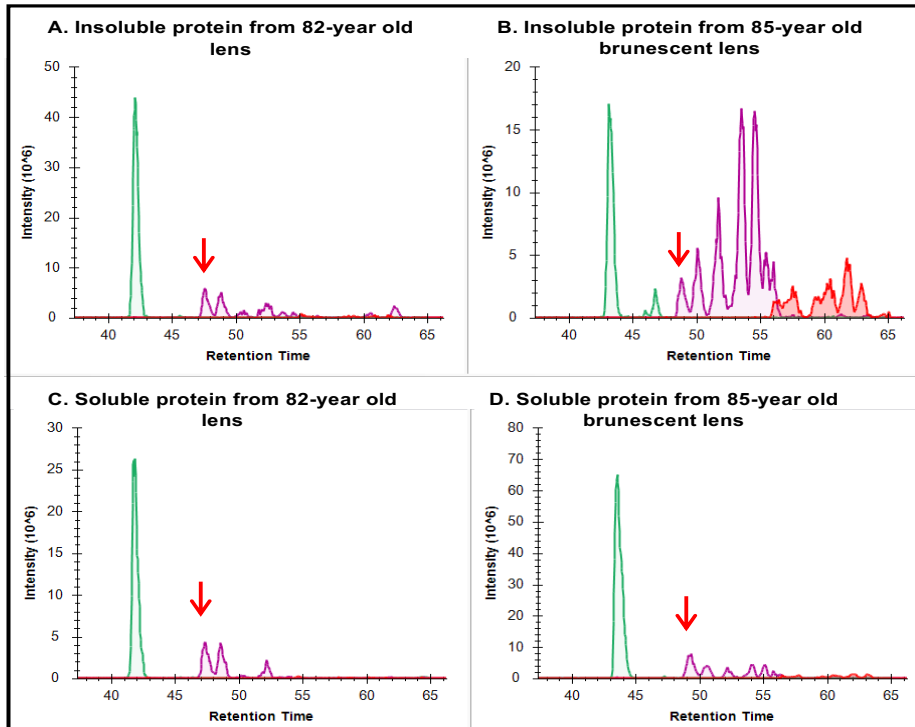


Figure S1. Chromatograms of doubly charged γ S peptide 7-18 (ITFYEDKNFQGR) isolated from 82- and 85-year old human lens nucleus. Chromatograms show the extent of deamidation in the water-soluble and water insoluble fractions. Non-deamidated (green), singly deamidated (purple), and doubly deamidated peptide (red). The arrow shows the peptide containing deamidation at only Q16, while all other singly deamidated forms contained deamidation at only N14. Note that the multiple peaks are due to isomerization and racemization occurring when N14 deamidates, as well as isomerization and racemization occurring at D12. The area under the singly deamidated purple peaks, not including the peak from the peptide with a deamidated Q16 (arrow), as well as the area under all doubly deamidated peaks were used to calculate the values for % deamidation at N14 shown in Fig. 2.

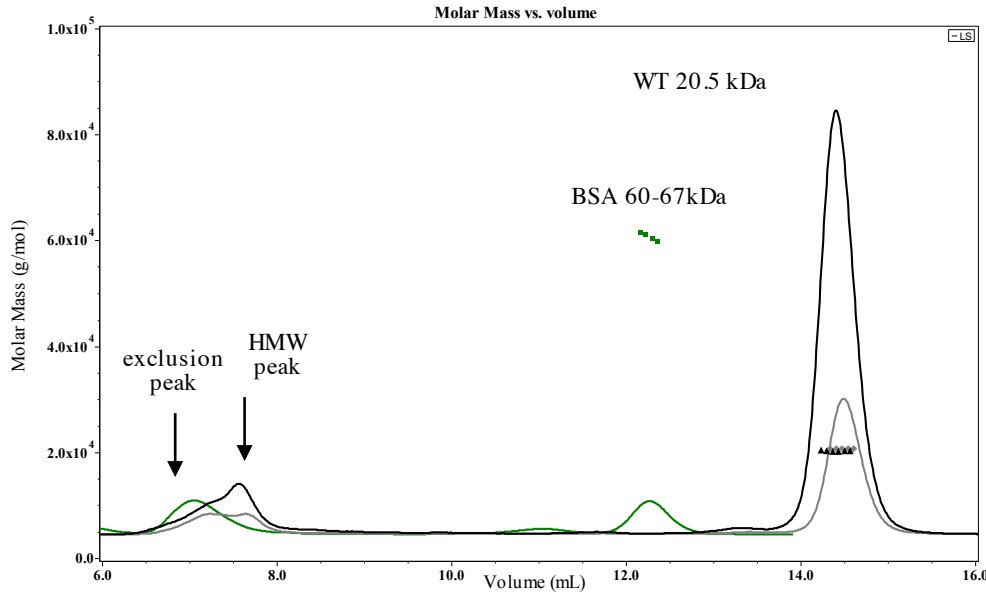
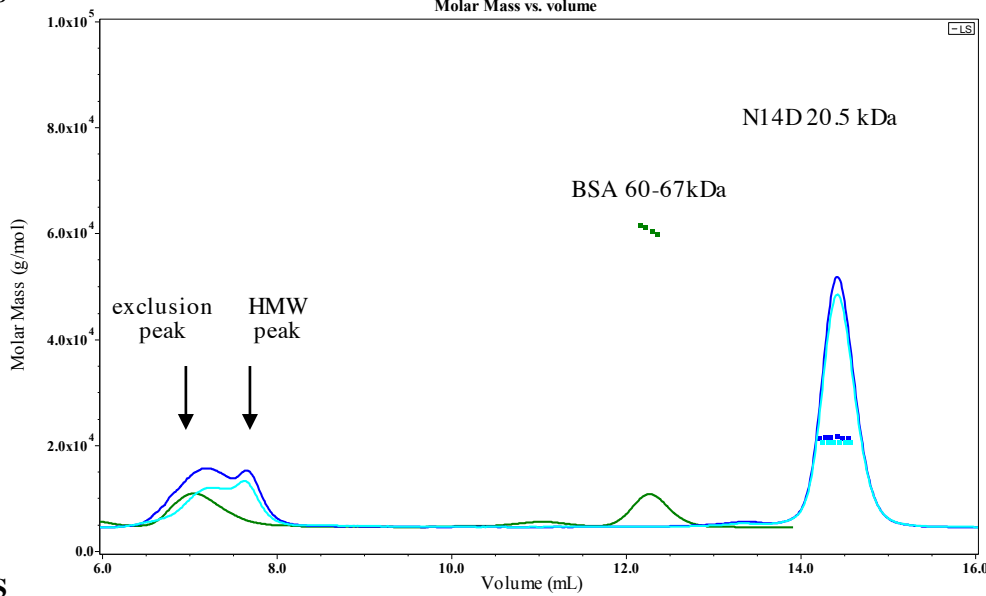
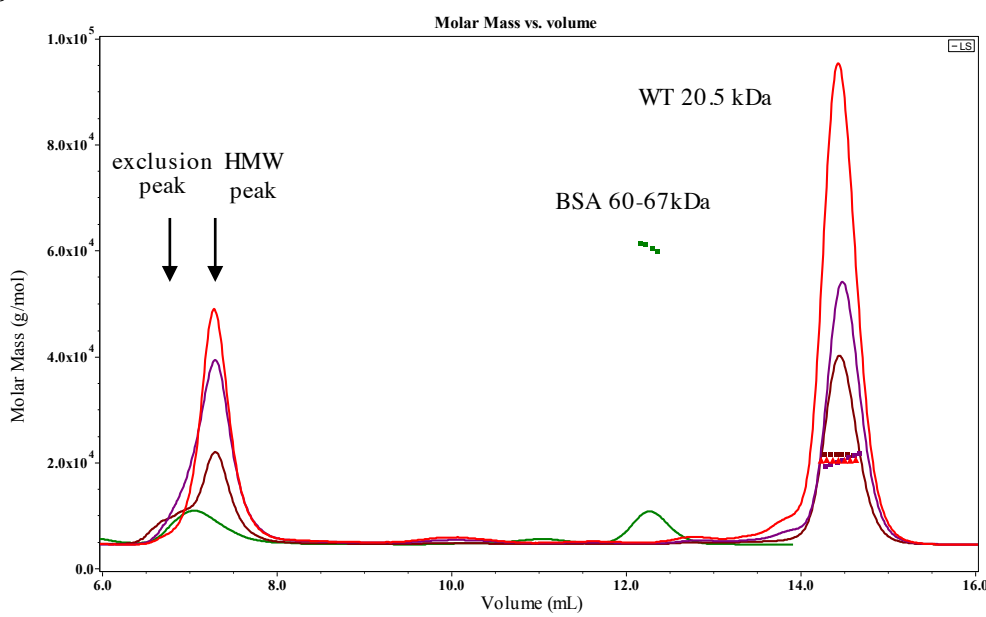
A. WT γ S**B. N14D γ S****C. N76D γ S**

Figure S2. Relative Rayleigh light scattering (LS tracings) and molar masses (markers) of WT and deamidated human γ S crystallins. (A) WT tracings (grey and black), **(B)** N14D tracings (cyan and blue), and **(C)** N76D tracings (purple, brown, and red) during size-exclusion chromatography in-line with multiangle laser scattering. The γ S monomer eluted between 14 and 15 mL for all three samples and was between 20-21 kDa. Different concentrations were injected with approximately 100-400 ug eluting in the monomer peaks. A 50 ug sample of bovine serum albumin (BSA) was used to determine the elution volume of the exclusion peak at 7 mls (black arrow and the green LS tracing). An additional light scattering peak just after this exclusion peak between 7-8 mls (blue arrow) was detected and had greater intensity in N14D and N76D than in WT at similar protein concentrations injected. All peak intensities are relative to the highest monomer peak intensity found in panel C.

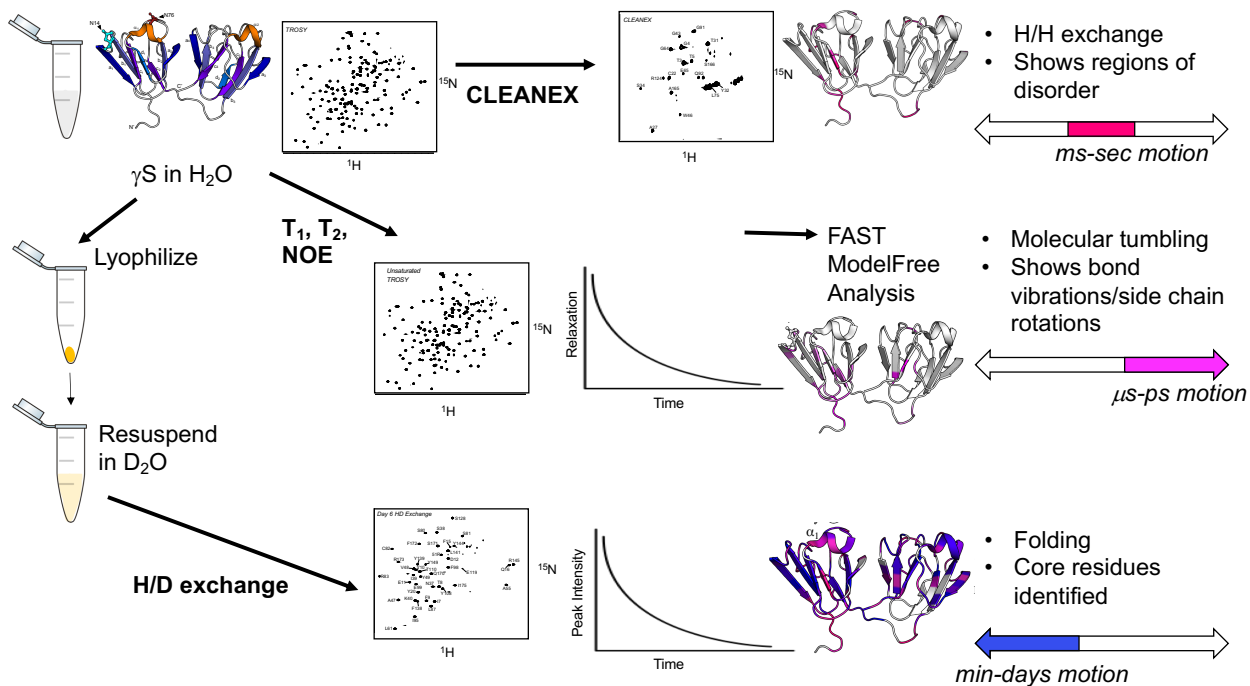


Figure S3. Summary of NMR methods. Experiments CLEANEX-HSQC, T1, T2, and 1H - ^{15}N Heteronuclear NOE were collected on WT, N14D, and N76D γ S crystallin to obtain dynamics information for ps-to-sec motions. Samples were then lyophilized and resuspended in D_2O to collect information about motions occurring on the timescale of min-to-days.

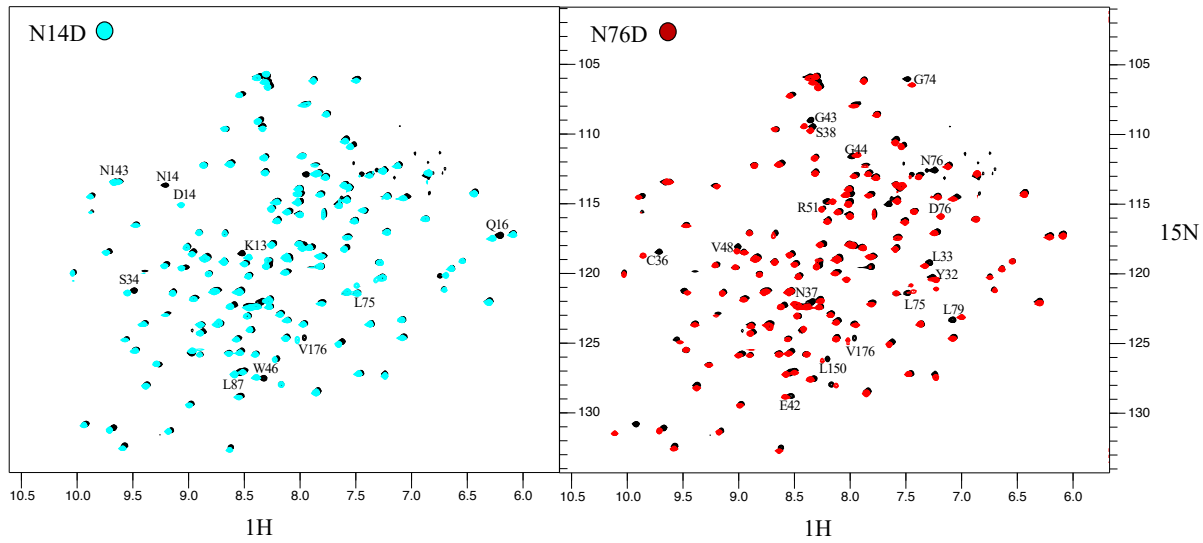


Figure S4. TROSY overlay of WT (black) with N14D (cyan) on the left and N76D (red) on the right. Spectra were referenced to DSS.

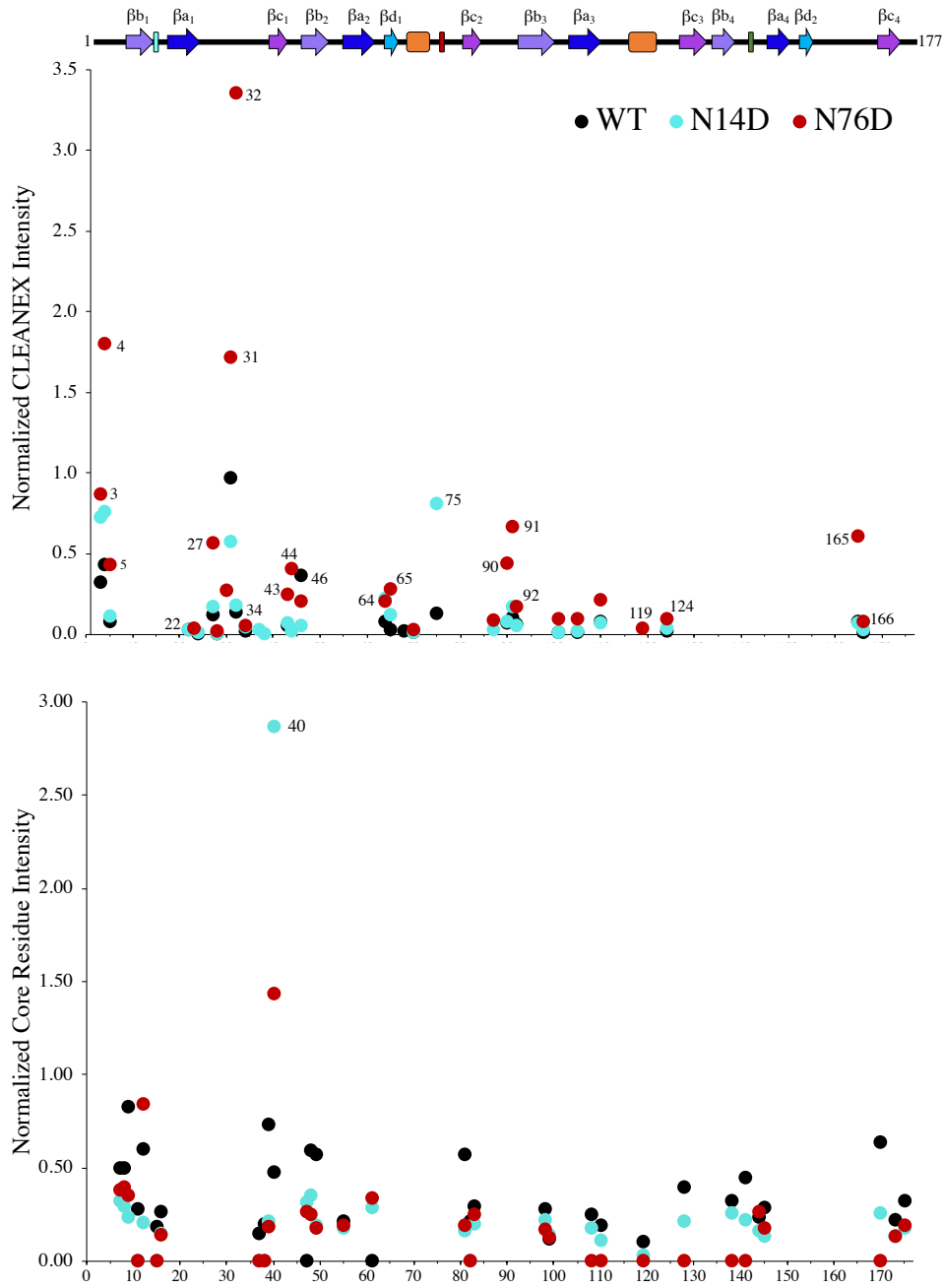


Figure S5. CLEANEX (top) and day 6 core residue (bottom) intensities of WT (black), N14D (cyan), and N76D (red). Values were normalized to the TROSY peak intensities, and presented as a ratio of CLEANEX or core residue intensities to TROSY intensities for the same residues in the same samples. Regions of high intensity that differ from WT were plotted in hotpink (CLEANEX) or blue (core residues) onto the structure in Figure 6A.

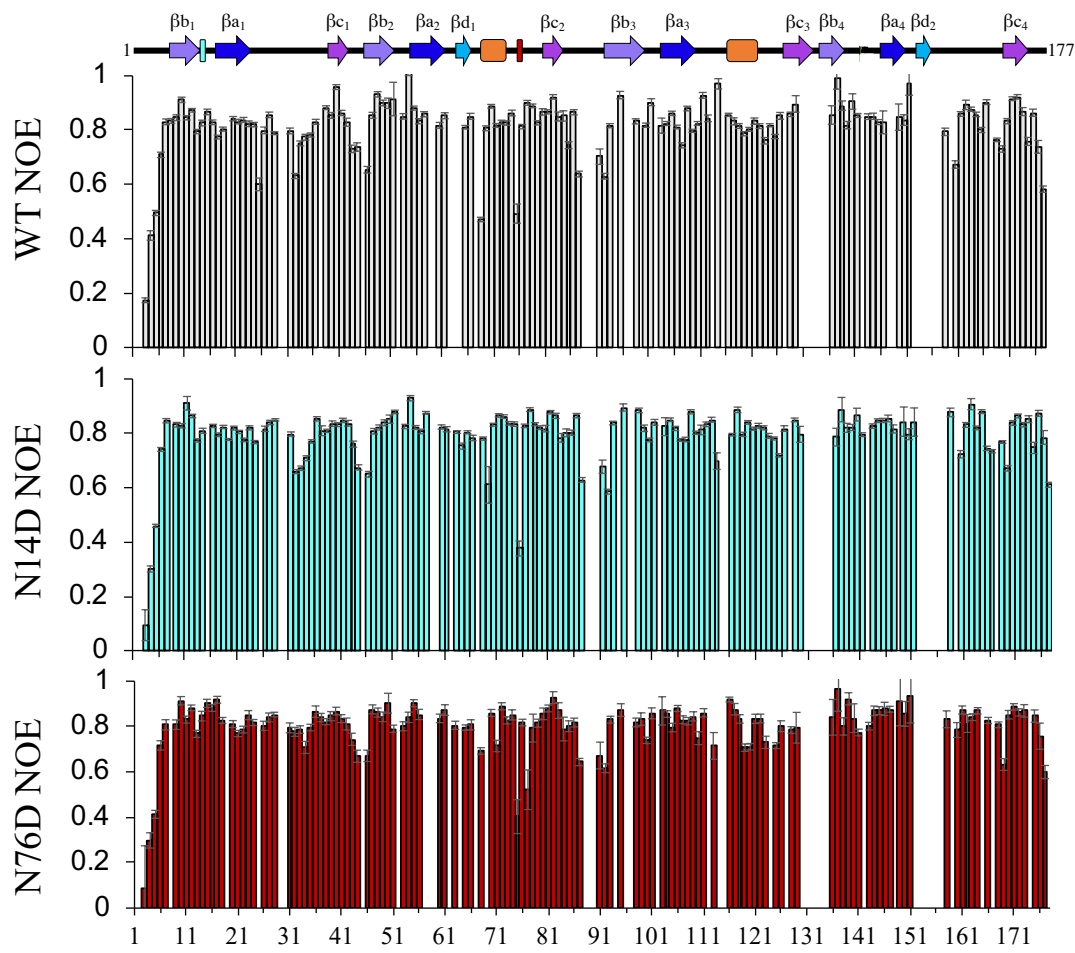


Figure S6. NOE values for WT (black), N14D (cyan), and N76D (red). Values below 0.5 indicated regions of flexibility while those close to 1.0 corresponded to fully ordered regions.

Residue	WT k_{α} (sec ⁻¹ *10 ⁻⁶)	N14D k_{α} (sec ⁻¹ *10 ⁻⁶)	N76D k_{α} (sec ⁻¹ *10 ⁻⁶)					
S2	500 ± 300	f	900 ± 400	V85	3 ± 8	7 ± 50	2 ± 0.013	
K6	400 ± 400	600 ± 700	900 ± 800	H86	0.05 ± 0.001	0.016 ± 0.001	0.09 ± 0.001	
I7	s	0.17 ± 0.006	400 ± 1100	G90	30 ± 12	40 ± 14	2 ± 0.003	
T8	s	0.3 ± 0.003	1500 ± 900	G91	x	300 ± 140	80 ± 6	
F9	s	s	0.13 ± 0.001	Y93	s	i	0.5 ± 0.001	
Y10	0.2 ± 0.001	s	19 ± 3	E99	90 ± 160	0.05 ± 0.001	s	
E11	0.3 ± 0.003	17 ± 2	5 ± 0.05	K100	s	30 ± 11	40 ± 7	
D12	0.2 ± 0.001	0.5 ± 0.0016	3 ± 0.001	F103	i	130 ± 30	f	
K13	s	s	0.5 ± 0.001	S104	s	130 ± 13	200 ± 60	
N14	i	s	200 ± 50	Q106	s	0.10 ± 0.001	f	
F15	0.4 ± 0.001	20 ± 0.4	0.6 ± 0.001	M107	0.12 ± 0.007	s	f	
Q16	0.07 ± 0.001	s	0.3 ± 0.002	Y108	0.17 ± 0.001	s	20 ± 11	
R18	s	1300 ± 900	f	T110	s	12 ± 20	s	
R19	500 ± 200	150 ± 500	900 ± 300	T111	s	i	6 ± 0.19	
Y20	s	s	6 ± 0.005	E112	500 ± 90	50 ± 11	s	
C22	x	x	50 ± 40	D113	f	f	300 ± 190	
D23	f	i	0.12 ± 0.001	C114	s	s	0.2 ± 0.001	
D25	700 ± 600	400 ± 200	5 ± 0.001	S116	0.07 ± 0.0014	s	16 ± 0.001	
C26	80 ± 120	60 ± 70	i	I117	1.5 ± 0.007	3 ± 0.006	f	
D28	x	x	400 ± 0.001	M118	0.04 ± 0.001	s	1.1 ± 0.001	
H30	800 ± 600	10 ± 7	x	E119	s	0.2 ± 0.001	f	
L33	160 ± 17	120 ± 4	600 ± 500	Q120	s	0.2 ± 0.001	0.08 ± 0.001	
R35	0.4 ± 0.001	800 ± 190	700 ± 700	H122	s	0.6 ± 0.004	f	
C36	1.4 ± 0.003	800 ± 200	1004 ± 1700	M123	600 ± 400	900 ± 900	f	
N37	60 ± 7	x	130 ± 65	R124	0.2 ± 0.001	12 ± 40	16 ± 4	
S38	0.2 ± 0.0014	x	0.003 ± 0.001	E125	s	s	0.03 ± 0.001	
K40	0.13 ± 0.001	s	0.12 ± 0.04	I126	i	40 ± 17	40 ± 100	
V41	7 ± 0.8	19 ± 40	20 ± 1.3	S128	0.06 ± 0.001	s	0.06 ± 0.001	
E42	s	s	0.19 ± 0.001	C129	20 ± 0.8	14 ± 1.0	i	
G43	120 ± 20	x	x	W136	4 ± 0.06	s	i	
T45	s	40 ± 2	1030 ± 0.001	I137	0.02 ± 0.001	0.4 ± 0.001	0.05 ± 0.001	
A47	s	s	0.06 ± 0.001	Y139	s	s	0.5 ± 0.006	
V48	0.08 ± 0.001	s	0.03 ± 0.001	E140	0.2 ± 0.001	6 ± 0.14	1.2 ± 0.007	
Y49	s	5 ± 0.3	2 ± 0.05	L141	s	0.8 ± 0.10	110 ± 0.001	
E50	s	s	1 ± 0.008	N143	40 ± 0.7	s	30 ± 19	
R51	s	0.16 ± 0.001	2 ± 0.008	Y144	s	s	0.3 ± 0.001	
N53	i	300 ± 40	600 ± 500	R145	s	0.3 ± 0.001	0.3 ± 0.02	
F54	0.2 ± 0.001	1.6 ± 0.3	0.7 ± 0.005	G146	0.2 ± 0.001	1.3 ± 0.04	5 ± 0.2	
A55	0.1 ± 0.001	s	0.5 ± 0.011	R147	500 ± 400	200 ± 140	i	
Y57	f	600 ± 180	2 ± 0.03	Y149	0.05 ± 0.001	s	0.12 ± 0.001	
I60	s	60 ± 7	100 ± 40	L150	i	200 ± 40	300 ± 400	
L61	s	s	0.03 ± 0.001	L151	0.013 ± 0.001	s	0.11 ± 0.001	
Y66	40 ± 40	s	s	K158	30 ± 11	s	130 ± 50	
E68	x	40 ± 110	100 ± 120	I160	1.2 ± 0.007	3 ± 0.008	i	
Y69	200 ± 70	f	800 ± 300	D161	110 ± 90	80 ± 7	80 ± 70	
R71	f	900 ± 1600	f	W162	i	19 ± 5	20 ± 2	
W72	3 ± 0.06	170 ± 13	7 ± 0	G163	s	300 ± 40	300 ± 70	
M73	0.4 ± 0.001	90 ± 1400	800 ± 700	A164	s	s	1.7 ± 0.001	
G74	s	700 ± 200	2 ± 0.018	S166	f	0.4 ± 0.06	2 ± 0.06	
N76	17 ± 0.4	1300 ± 1100	600 ± 300	V169	4 ± 0.02	1200 ± 800	0.14 ± 0.001	
D77	s	i	1.3 ± 0.04	Q170	4 ± 0.19	s	2 ± 0.015	
R78	s	150 ± 6	i	S171	0.06 ± 0.001	s	4 ± 0.4	
L79	0.8 ± 0.008	110 ± 11	s	F172	17 ± 0.14	1 ± 0.001	s	
S80	400 ± 400	s	0.5 ± 0.07	R173	s	s	9 ± 0.5	
S81	0.2 ± 0.002	s	s	R174	700 ± 300	50 ± 60	s	
C82	0.2 ± 0.001	s	80 ± 200	I175	4 ± 1.7	60 ± 60	1.4 ± 0.8	
R83	0.02 ± 0.001	s	0.4 ± 0.012	V176	0.4 ± 0.001	i	f	
A84	140 ± 60	90 ± 8	5 ± 0.06	E177	s	0.11 ± 0.001	s	

Table S1. Measured H/D exchange rates for WT (grey), N14D (cyan), and N76D (red). For residues in which H/D exchange rates could not be determined, ‘s’ was used to denote slow exchanging protons which did not experience appreciable decay after 6 days, ‘i’ for those that exchanged on an intermediate timescale between 2-6 days, ‘f’ for fast exchanging residues which exchanged after 1 day, and ‘x’ for those residues that appear in CLEANEX spectra and are the most rapidly exchanging.